JOURNAL OF COMPUTATIONAL PHYSICS 117, 228–239 (1995)

Direct Computation of Boundary-Layer Stability Characteristics

J. A. MASAD AND M. R. MALIK

High Technology Corporation, Hampton, Virginia 23666

Received October 22, 1993; revised August 1, 1994

A method is presented for the direct and efficient computation of certain characteristics of differential eigenvalue problems. The method is based on the differentiation of the governing equations with respect to one or more of the parameters of the associated dispersion relation. The new problem (or problems), coupled with the original problem, is solved to directly compute a certain required characteristic (e.g., the maximum disturbance growth rate). The method is applied to two problems in boundary-layer stability: the viscous instability of incompressible flow over a flat plate with suction and the inviscid instability of compressible flow over a flat plate with different wall and flow conditions. The new method has potential applications in both computational physics and engineering. © 1995 Academic Press, Inc.

1. INTRODUCTION

The study of the stability of boundary layer flows in the context of linear theory gives rise to various instabilities such as Tollmien–Schlichting (T–S), Görtler, crossflow, attachment-line, and secondary instabilities (see for example Malik [1]). When the normal-mode approach (see for example Mack [2], Malik [3]) is used to analyze such instabilities, the common mathematical framework constitutes a system of differential eigenvalue problems. These eigenvalue problems have, in general, various free parameters such as the frequency of the disturbance, the components of the wave-number vector, the growth rate components, the Reynolds number, the Görtler number, and the amplitude of the primary disturbance in secondary instabilities. The free parameters in a certain eigenvalue problem are related through the dispersion relation (or relations), which for the stability problem under discussion is not known analytically. To understand the response of boundary-layer flow to various instabilities, the interrelationships between the parameters of the associated dispersion relation (or relations) must be understood.

For a boundary-layer stability problem, the variation of a disturbance growth rate with various parameters of the associated dispersion relation or with flow conditions can be studied. To describe the effect of a certain parameter as stabilizing or destabilizing, the effect on the maximum growth rate over all values of one or more parameters of the dispersion relation is considered. For example, suction can increase or decrease the growth rate of a fixed-frequency second-mode wave in hypersonic flow over a flat plate. However, suction stabilizes second-mode waves because it decreases the maximum growth rate over all frequencies. This indicates the need to compute certain stability characteristics, such as maximum growth rate or neutral points, accurately and efficiently. In this paper, we present a new general method that can be used to directly and efficiently compute certain characteristics related to the eigenvalue problem. For example, we will show how the maximum growth rate can be computed as part of the solution. In Section 2, we outline the method. In Section 3, we apply the method to two sample problems from the stability of boundary layers. Finally, in Section 4, we summarize the findings.

2. GENERAL OUTLINE OF THE METHOD

In the linear quasi-parallel stability analysis, the normal-mode form of the solution is used to separate the temporal, streamwise spatial, and spanwise spatial dependencies (see for example Mack [2]). A fluctuation quantity q is expressed as

$$q = \zeta(y)e^{i(\alpha x+\beta z-\omega t)} + cc, \tag{1}$$

where x is the streamwise coordinate, y is the normal coordinate, z is the spanwise coordinate, and t is the time. The function ζ is complex, and cc denotes the complex conjugate of the preceding term. The parameters α, β, and ω are complex in general. In temporal stability analyses, α (real) is the disturbance streamwise wave number, and β (real) is the disturbance spanwise wave number. The real part of ω, (denoted by ω_r), is the disturbance frequency, and the imaginary part of ω, (denoted by ω_i), is the temporal disturbance growth rate. In spatial stability analyses, ω (real) is the disturbance frequency, the real parts of α and β (α_r and β_r) are the disturbance streamwise and spanwise wave numbers, respectively, and the imaginary parts of α and β (α_i and β_i) are the disturbance streamwise and spanwise rates of decay, respectively. By substituting Eq.

0021-9991/95 $6.00

(1) in the linearized Navier–Stokes equations, the resulting homogeneous ordinary differential equations can be written as a system of first-order equations. Homogeneous boundary conditions associated with the governing equations result in an eigenvalue problem. If the equations are written in complex variables, then the resulting system has a single complex dispersion relation (two real relations); therefore, in principle, the real and imaginary parts of all the free parameters in the system can be specified, except for two real parameters which can be determined.

The system of first-order complex ordinary differential equations is expressed as

$$D\{\zeta\} = [F](q_m; \alpha, \alpha^2, ..., \beta, \beta^2, ..., \omega, R, G, A, ...)\{\zeta\}, \quad (2)$$

where

$$D = d/dy$$

and q_m are mean-flow quantities that are generally functions of y. The parameters R, G, A, ... are other free parameters that can occur in certain stability eigenvalue problems. For example, R can be the local Reynolds number, G can be the Görtler number, and A can be the disturbance amplitude in a certain wave-interaction problem such as the amplitude of the primary wave in secondary instability or the amplitude of the Tollmien–Schlichting (T–S) wave in a T–S–Görtler wave-interaction problem. If we have n complex equations, then ζ is a column vector with n complex components and F is a square matrix of order $n \times n$ with complex elements. Associated with system (2) are m ($m < n$) homogeneous boundary conditions at one boundary (boundary I) and $n - m$ boundary conditions at boundary II. Because ζ is complex and in the presence of a single complex dispersion relation, a normalization condition can be used. Without loss of generality, assume that the normalization condition is

$$\zeta_k = c \quad \text{at boundary I,} \quad (3)$$

where c is any nonzero complex number. Equation (2) and the boundary conditions at boundaries I and II can be solved by assuming the real and imaginary parts of the all free parameters α, β, ω, R, ... (except for two); replacing one of the homogeneous complex boundary conditions at boundary I by the inhomogeneous boundary condition in Eq. (3); solving the resulting system for initial guesses for the two sought free parameters; and updating the value of two free parameters to satisfy the replaced homogeneous boundary condition at boundary I, and so on, until the two sought free parameters do not change within a preset tolerance.

A second approach for computing the two free parameters is to augment the system of equations (2) by two trivial, real differential equations that result from setting the derivative of each of the two free parameters with respect to y to zero. This change increases the order of the system of real differential equations from $2n$ to $2n + 2$, because the two free parameters are now treated as dependent variables, the resulting system is nonlinear. The nonlinear $2n + 2$ real homogeneous system of differential equations can be solved subject to the $2m$ real homogeneous boundary conditions at boundary I, $2n - 2m$ real homogeneous boundary conditions at boundary II, and the two real boundary conditions (at least one of the 2 is inhomogeneous) that result from the normalization condition (3). The required two free parameters are part of the solution.

The procedure described in the above paragraph can be used to directly compute important stability characteristics such as neutral curves or threshold amplitudes of excitation in wave-interaction problems. For example, to compute neutral curves for two-dimensional disturbances ($\beta = 0$) in two-dimensional boundary-layer flow over a flat plate, set $\omega_i = \alpha_i = 0$, specify ω_r, and compute α_r and R. To do the same for three-dimensional disturbances ($\beta \neq 0$) in two-dimensional boundary-layer flow over a flat plate ($\beta_i = 0$), β_r, must be specified $\omega_i = \alpha_i = 0$, must be set and α_r and R must be computed. However, the direct computation of the outmost neutral curves (over all values of β_r) with the above procedure is not possible. Furthermore, the computation of the maximum spatial growth rate, over all frequencies or over frequencies and spanwise wave numbers in two-dimensional flow, is not possible. We will shortly describe a procedure that allows the direct computation of these quantities.

Equation (2) can be differentiated with respect to ω as

$$D\left\{\frac{\partial \zeta}{\partial \omega}\right\} = \left[\frac{\partial F}{\partial \omega}\right]\left(q_m; \frac{\partial \alpha}{\partial \omega}, 2\alpha\frac{\partial \alpha}{\partial \omega}, ..., \frac{\partial \beta}{\partial \omega}, 2\beta\frac{\partial \beta}{\partial \omega}, ..., 1, \frac{\partial R}{\partial \omega}, \frac{\partial G}{\partial \omega}, \frac{\partial A}{\partial \omega}, ...\right)\{\zeta\} + [F](q_m, \alpha, \alpha^2, ..., \beta, \beta^2, ..., \omega, R, G, A, ...)\left\{\frac{\partial \zeta}{\partial \omega}\right\}. \quad (4)$$

If the system given by Eq. (2) has n complex differential equations and m homogeneous boundary conditions at boundary II, then the same is true for the system given by Eqs. (4). Although system (2) is decoupled from system (4), the opposite is not true. Systems (2) and (4) together have $2n$ complex differential equations, $2m$ boundary conditions at boundary I, and $2n - 2m$ boundary conditions at boundary II. System (2), treated as a nonlinear system, has the dependent variables α, β, ..., and system (4) introduces additional dependent variables ($\partial\alpha/\partial\omega$, $\partial\beta/\partial\omega$, ...). Systems (2) and (4) are augmented by the trivial equation

$$D\alpha = D\beta = \cdots = D\frac{\partial \alpha}{\partial \omega} = D\frac{\partial \beta}{\partial \omega} = \cdots = 0.$$

A normalization condition similar to (3) can be used; thus,

$$\frac{\partial \zeta_k}{\partial \omega} = c. \tag{5}$$

Furthermore, system (4) introduces a second complex dispersion relation, in addition to the one introduced by system (2).

With the system given by Eqs. (2)–(5), stability characteristics such as the maximum spatial growth rate of two-dimensional disturbances in two-dimensional compressible flow over a flat plate at a fixed Reynolds number can now be computed directly. For this case, both systems (2) and (4) introduce six complex differential equations; thus, 12 complex equations are introduced. Other equations are

$$D\alpha = D\omega = D\frac{\partial \alpha}{\partial \omega} = 0.$$

If ω and α are treated as complex, then 15 complex differential equations with 15 complex variables exist, and 30 real boundary conditions are required. System (2) gives three complex homogeneous boundary conditions at boundary I and three more at boundary II; the same is true for system (4), which results in 24 real boundary conditions. The normalization conditions (3) and (5) give four more real boundary conditions, which results in a total of 28 real boundary conditions. Because ω is real in spatial stability analysis, the 29th condition is $\omega_i = 0$. The system can be closed by requiring that the spatial growth rate α_i is maximum over all frequencies (i.e., $\partial\alpha_i/\partial\omega = 0$). Hence, the solution we compute for α_r, ω, and $\partial\alpha_r/\partial\omega$ (the reciprocal of the group velocity) corresponds to the maximum growth rate $-\alpha_i$. Note that the computations yield four free parameters because the coupled system has two complex (four real) dispersion relations.

If system (2) is differentiated with respect to β, then

$$D\left\{\frac{\partial \zeta}{\partial \beta}\right\} = \left[\frac{\partial F}{\partial \omega}\right]\left(q_m, \frac{\partial \alpha}{\partial \beta}, 2\alpha\frac{\partial \alpha}{\partial \beta}, ..., 1, 2\beta, ..., \frac{\partial \omega}{\partial \beta}, \frac{\partial R}{\partial \beta}, \frac{\partial G}{\partial \beta}, \frac{\partial A}{\partial \beta}, ...\right)\{\zeta\} + [F](q_m, \alpha, \alpha^2, ..., \beta, \beta^2, ..., \omega, R, G, A, ...)\left\{\frac{\partial \zeta}{\partial \beta}\right\}. \tag{6}$$

The resulting system (coupled with system (2)), the associated trivial differential equations, and the boundary conditions can be used to directly compute additional stability characteristics. For example, the maximum spatial growth rates over all values of β of three-dimensional disturbances in two-dimensional compressible flow over a flat plate at a fixed ω and R can be computed from these systems. Systems (2), (4), and (6) together can be used to directly compute additional stability characteristics. For example, if we consider three-dimensional disturbances in two-dimensional compressible flow over a flat plate, then the three systems result in 24 complex differential equations. At the same R, the additional trivial equations are

$$D\alpha = D\beta = D\omega = D\frac{\partial \alpha}{\partial \omega} = D\frac{\partial \alpha}{\partial \beta} = 0.$$

Note that

$$\frac{\partial \omega}{\partial \beta} = \frac{\partial \omega}{\partial \alpha}\frac{\partial \alpha}{\partial \beta} = \frac{\partial \alpha}{\partial \beta}\Big/\frac{\partial \alpha}{\partial \omega}$$

and

$$\frac{\partial \beta}{\partial \omega} = 1\Big/\left(\frac{\partial \omega}{\partial \beta}\right)$$

which results in 29 complex differential equations. Systems (2), (4), and (6) have 24 complex (48 real) homogeneous boundary conditions. The normalization conditions introduce 6 real boundary conditions with a total of 54 real boundary conditions. For spatial stability, $\omega_i = 0$, which results in 55 real boundary conditions. For two-dimensional flow, and to compute the maximum growth rate over all frequencies and spanwise wave numbers, the remaining three boundary conditions are

$$\beta_i = 0, \quad \frac{\partial \alpha_i}{\partial \omega} = \frac{\partial \alpha_i}{\partial \beta} = 0.$$

In a three-dimensional flow over an infinite swept-wing, with the assumption that $\beta_i = 0$, the envelope method is implemented by setting

$$\beta_i = \frac{\partial \alpha_i}{\partial \omega} = \frac{\partial \alpha_i}{\partial \beta} = 0$$

just as in the previously considered two-dimensional case.

In the above example, if we use

$$\omega_i = \beta_i = \frac{\partial \alpha_i}{\partial \omega} = \frac{\partial \alpha_i}{\partial \beta} = 0$$

directly in the equations and not as additional conditions, then the order of the system of equations is reduced from 58 real differential equations to 54 real differential equations. However, by assuming all the quantities in the equations to be complex, the resulting equations and the associated Jacobian have a structure that allows them to be easily split into real and imaginary parts. This approach is convenient for the solution method used in these applications.

If system (2) is differentiated with respect to α, then some stability characteristics can be computed directly in the context of temporal stability theory. The group velocity that is part of the solution can then be used to convert the temporal growth rates into spatial growth rates. System (2) can also be differentiated with respect to R, and, from the resulting coupled system, other stability characteristics can be computed, such as the maximum growth rate over all values of R. We foresee many other possible extensions of the outlined method for directly computing other stability characteristics in both simple and complicated flows. Furthermore, the method in its general form is not restricted to hydrodynamic instability problems, but can be applied to any eigenvalue problem. In that case, differentiating the eigenvalue problem with respect to the various parameters of the dispersion relation (or relations) might result in a coupled system that can be used to directly compute some significant characteristics of the eigenvalue problem under consideration.

3. APPLICATIONS

In this section, we apply the previously outlined method to two sample problems. The first problem is the viscous instability of incompressible flow over a flat plate, and the second problem is the inviscid instability of compressible flow over a flat plate. In both problems, the application of the method in order to compute the maximum growth rate over all frequencies is demonstrated. The results for the first problem show the maximum growth rates as they vary with Reynolds number at various levels of suction. For the second problem, the results show the effect of heat transfer, suction, and free-stream temperature on the maximum growth rates of second-mode waves at various Mach numbers.

3.1. *Viscous Instability of Incompressible Flow over a Flat Plate*

The incompressible mean flow over a flat plate with self-similar suction is governed by the equation (see for example Asfar *et al.* [4])

$$\frac{d^2U}{d\phi^2} + g\frac{dU}{d\phi} = 0, \tag{7}$$

where

$$g = -V_w + \frac{1}{2}\int_0^\phi U\, d\phi \tag{8}$$

and

$$\phi = y\sqrt{\frac{\mathrm{Re}}{x}} \tag{9}$$

The boundary conditions are

$$U = 0, g = V_w \quad \text{at } \phi = 0 \tag{10}$$

$$U \to 1 \quad \text{as } \phi \to \infty, \tag{11}$$

where

$$V_w = \sqrt{x\,\mathrm{Re}}\,\frac{v_w^*}{U_\infty^*} \tag{12}$$

and

$$\mathrm{Re} = \frac{U_\infty^* L^*}{\nu^*} \tag{13a}$$

$$(x, y) = \frac{(x^*, y^*)}{L^*} \tag{13b}$$

$$U = \frac{U^*}{U_\infty^*} \tag{13c}$$

In the above equations, x and y are the nondimensional streamwise and normal coordinates, respectively, made nondimensional with respect to a constant reference length L^*. The streamwise nondimensional velocity U is made nondimensional with respect to the free-stream velocity U_∞^*. The free-stream Reynolds number is Re, ν^* is the kinematic viscosity, and v_w^* is the dimensional transverse suction velocity at the wall. The suction velocity v_w^* and, consequently, V_w are negative for suction and positive for blowing.

The quasi-parallel stability of the flow is formulated by using the normal-mode form given by Eq. (1). For only two-dimensional disturbances, we let

$$(u, v, p) = (\zeta_1, \zeta_3, \zeta_4)e^{i(\alpha x - \omega t)} + cc \tag{14}$$

If Eq. (14) is substituted into the linearized quasi-parallel disturbance equations (see for example Asfar et al. [4]), which are derived from the Navier–Stokes equations, then we obtain

$$i\alpha\zeta_1 + D\zeta_3 = 0 \tag{15}$$

$$-\frac{1}{R}D^2\zeta_1 + \frac{\Gamma}{R}\zeta_1 + DU\zeta_3 + i\alpha\zeta_4 = 0 \tag{16}$$

$$-\frac{1}{R}D^2\zeta_3 + \frac{\Gamma}{R}\zeta_3 + D\zeta_4 = 0. \tag{17}$$

where

$$\Gamma = \alpha^2 + iR(\alpha U - \omega) \tag{18a}$$

$$R = \frac{U_\infty^* \delta_r^*}{\nu^*} \tag{18b}$$

$$\delta_r^* = \sqrt{\frac{\nu^* x^*}{U_\infty^*}} \tag{18c}$$

and $D = \partial/\partial\eta$. In the above equations, we have

$$\eta = \frac{y^*}{\delta_r^*}. \tag{19}$$

The parameters α and β are complex in general. The boundary conditions are

$$\zeta_1 = \zeta_3 = 0 \quad \text{at } \eta = 0 \tag{20}$$

$$\zeta_n \to 0 \quad \text{as } \eta \to \infty \tag{21}$$

Eqs. (15)–(17) can be rewritten as a system of first-order differential equations in the form

$$D\{\zeta\} = [F]\{\zeta\}, \tag{22}$$

where

$$\{\zeta\} = \{\zeta_1, \zeta_2, \zeta_3, \zeta_4\}^T \tag{23a}$$

and

$$\zeta_2 = D\zeta_1 \tag{23b}$$

The complex elements of the 4×4 matrix F are given in Appendix A.

If Eqs. (20)–(22) are differentiated with respect to ω, we get

$$D\left\{\frac{\partial\zeta}{\partial\omega}\right\} = \left[\frac{\partial F}{\partial\omega}\right]\{\zeta\} + [F]\left\{\frac{\partial\zeta}{\partial\omega}\right\} \tag{24}$$

$$\frac{\partial\zeta_1}{\partial\omega} = \frac{\partial\zeta_3}{\partial\omega} = 0 \quad \text{at } \eta = 0 \tag{25}$$

and

$$\frac{\partial\zeta_n}{\partial\omega} \to 0 \quad \text{as } \eta \to \infty \tag{26}$$

where $\partial F/\partial\omega$ is a 4×4 matrix with its elements generated by differentiating the elements of F with respect to ω. This differentiation gives rise to the quantities $\partial\alpha/\partial\omega$ and $\partial R/\partial\omega$. If we are interested in performing calculations at a fixed Reynolds number R, then $\partial R/\partial\omega$ is set to 0. Equations (20)–(22) are decoupled from Eqs. (24)–(26), but the opposite is not true. If α, ω, and $\partial\alpha/\partial\omega$ are treated as dependent variables, then Eqs. (22) and (24) can be rewritten as a system of first-order differential equations as

$$\{\xi\} = \left\{\zeta_1, \zeta_2, \zeta_3, \zeta_4, \frac{\partial\zeta_1}{\partial\omega}, \frac{\partial\zeta_2}{\partial\omega}, \frac{\partial\zeta_3}{\partial\omega}, \frac{\partial\zeta_4}{\partial\omega}, \alpha, \omega, \frac{\partial\alpha}{\partial\omega}\right\}^T \tag{27a}$$

and

$$\{\xi\} = \{\xi_1, \xi_2, \xi_3, \xi_4, \xi_5, \xi_6, \xi_7, \xi_8, \xi_9, \xi_{10}, \xi_{11}\}^T. \tag{27b}$$

Then, we have

$$D\{\xi\} = [H]\{\xi\}, \tag{28}$$

where H is an 11×11 matrix of complex elements with its nonzero elements given in Appendix B. The system of Eq. (28) has 11 complex differential equations; to close the system we need 22 real boundary conditions. The boundary conditions (20) and (25) are rewritten as

$$\xi_1 = \xi_3 = \xi_5 = \xi_7 = 0 \quad \text{at } \eta = 0 \tag{29}$$

to supply eight real conditions. The boundary conditions (21) and (26) supply eight additional real asymptotic conditions in the free stream, which are implemented numerically by solving the constant coefficients system (28) in the free stream, inverting the eigenfunctions matrix, and demanding the boundedness of the disturbances in the free stream. Four more boundary conditions follow from the normalization conditions, which we choose as

$$\xi_2 = \xi_6 = 1 \quad \text{at } \eta = 0 \tag{30}$$

The result is a total of 20 boundary conditions. Two additional conditions are provided by requiring that

$$\omega_i = \text{Imag}(\xi_{10}) = 0 \tag{31}$$

$$\frac{\partial\alpha_i}{\partial\omega} = \text{Imag}(\xi_{11}) = 0 \tag{32}$$

where Imag denotes the imaginary part of a complex quantity.

To solve the system (28) and the associated boundary conditions, our choice of solution method must split the governing equations and boundary conditions into real and imaginary parts; the Jacobian of the system (28) must be derived and split into real and imaginary parts. Note here that the complex system (28) can be easily split numerically into real and imaginary parts as

$$\begin{Bmatrix} D\xi_r \\ D\xi_i \end{Bmatrix} = \begin{bmatrix} H_r & -H_i \\ H_i & H_r \end{bmatrix} \begin{Bmatrix} \xi_r \\ \xi_i \end{Bmatrix} \tag{33}$$

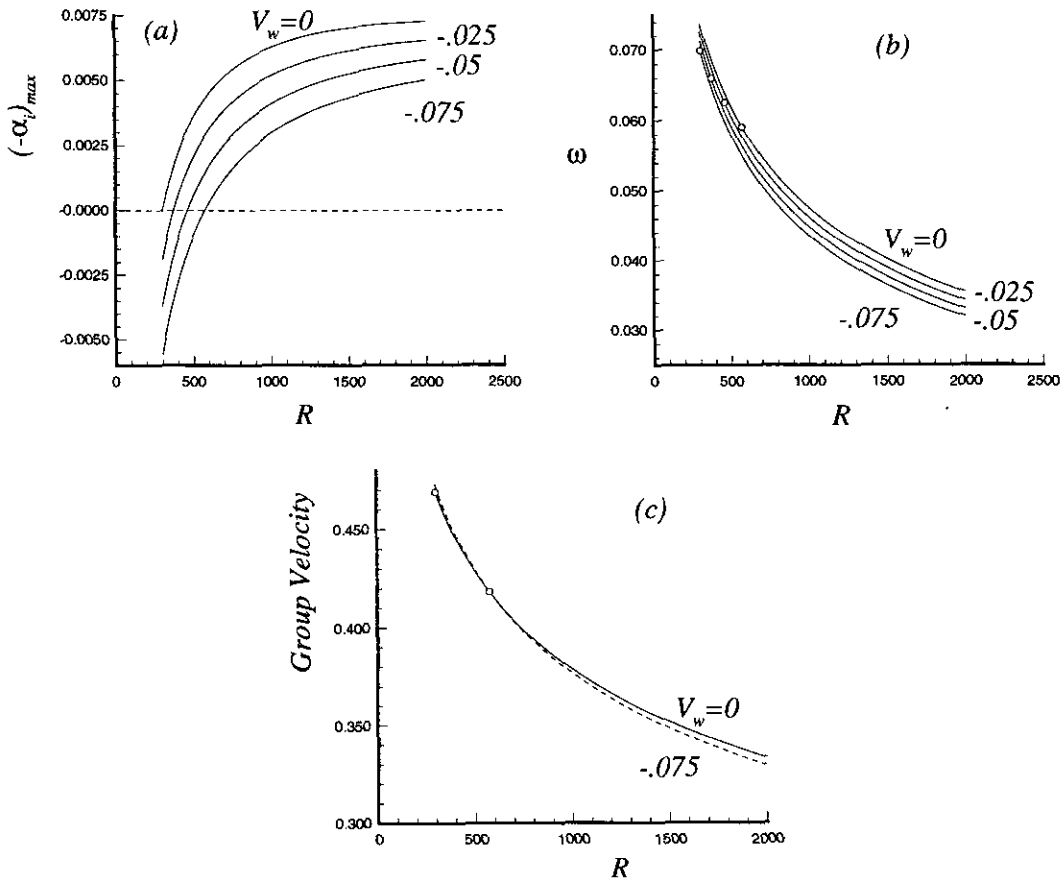

FIG. 1. (a) Variation of maximum growth rate with Reynolds number for four levels of self-similar suction. (b) Corresponding frequencies. (c) Group velocities.

The associated boundary conditions are split similarly. The complex Jacobian J of the complex system (28) has the complex elements J_{kj}, where

$$J_{kj} = \frac{\partial(D\xi_k)}{\partial \xi_j} \tag{34}$$

and its elements are given in Appendix C. The real Jacobian JJ has the structure

$$[JJ] = \begin{bmatrix} J_{rr} & J_{ri} \\ J_{ir} & J_{ii} \end{bmatrix} = \begin{bmatrix} \text{Real}\,(J) & -\text{Imag}(J) \\ \text{Imag}(J) & \text{Real}(J) \end{bmatrix} \tag{35}$$

The resulting nonlinear system of real differential equations, nonlinear real boundary conditions, and the nonlinear real Jacobian is supplied to the IMSL subroutine BVPFD [5], which solves a nonlinear, two-point boundary value problem. The subroutine is based on the code PASVA3, which uses finite differences with deferred correction. As a result of the solution we compute α, ω, and $\partial\alpha/\partial\omega$ to correspond to the maximum spatial growth rate over all frequencies ω. At the maximum growth rate $\partial\alpha/\partial\omega$, the reciprocal of the group velocity and, consequently, the group velocity are real. Note also that as part of the solution we compute four real, free parameters (α complex, ω real, and $\partial\alpha/\partial\omega$ real) because the system (24) has introduced a second complex dispersion relation, in addition to the original complex dispersion relation of system (22).

We solved the considered problem to compute the maximum spatial growth rates as a function of R at four levels of self-similar suction. The maximum spatial growth rates are shown in Fig. 1a, and the corresponding frequencies and group velocities are shown in Figs. 1b and 1c, respectively.

The central processing unit (CPU) time required to solve the 22 real, nonlinear differential equations for computing maximum disturbance growth rate is about three times the CPU time required to solve the original eight real, linear differential equations for one eigenvalue (not a maximum). The CPU time required to solve the maximum via indirect method depends upon the separation between the known eigenvalue and the desired eigenvalue, but clearly the direct approach saves scientist time. The results of direct computation of the maximum disturbance growth rate are in perfect agreement with the results of the indirect computations.

3.2. *Inviscid Instability of Compressible Flow over a Flat Plate*

The compressible mean flow over a flat plate with self-similar suction is governed by the equations (see for example Asfar *et al.* [4])

$$\frac{d}{d\phi}\left(\rho\mu\frac{dU}{d\phi}\right)+g\frac{dU}{d\phi}=0 \tag{36}$$

$$\frac{1}{\mathrm{Pr}}\frac{d}{d\phi}\left(\rho\mu\frac{dT}{d\phi}\right)+g\frac{dT}{d\phi}+(\gamma-1)M_\infty^2\rho\mu\left(\frac{dU}{d\phi}\right)^2=0 \tag{37}$$

$$g=-V_w+\frac{1}{2}\int_0^\phi U\,d\phi \tag{38}$$

$$\phi=\sqrt{\frac{\mathrm{Re}}{x}}\int_0^y\rho\,dy \tag{39}$$

The boundary conditions for the adiabatic wall are

$$U=\frac{dT}{d\phi}=0 \text{ and } g=-V_w \quad \text{at } \phi=0. \tag{40a}$$

For a wall with heat transfer,

$$U=0,\quad g=-V_w,\quad \text{and}\quad \frac{T_w}{T_{ad}} \text{ is specified at } \phi=0 \tag{40b}$$

In the free stream, the boundary conditions are

$$U\to 1,\ T\to 1 \quad \text{as } \phi\to\infty, \tag{41}$$

where

$$\mathrm{Pr}=\frac{\mu_\infty^* C_p^*}{\kappa_\infty^*} \tag{42a}$$

$$\mathrm{Re}=\frac{U_\infty^* L^*}{\nu_\infty^*} \tag{42b}$$

$$M_\infty=\frac{U_\infty^{*2}}{(\gamma-1)C_p^* T_\infty^*} \tag{42c}$$

$$V_w=\sqrt{x\,\mathrm{Re}}\,\frac{1}{T_w}\frac{v_w^*}{U_\infty^*} \tag{42d}$$

$$(x,y)=\frac{(x^*,y^*)}{L^*} \tag{42e}$$

$$U=\frac{U^*}{U_\infty^*},\ T=\frac{T^*}{T_\infty^*} \tag{42f}$$

$$(\rho,\mu,\nu)=\left(\frac{\rho^*}{\rho_\infty^*},\frac{\mu^*}{\mu_\infty^*},\frac{\nu^*}{\nu_\infty^*}\right) \tag{42g}$$

In the above equation, x and y are the nondimensional streamwise and normal coordinates, respectively, made nondimensional with respect to a constant reference length L^*. The streamwise nondimensional velocity U is made nondimensional with respect to the free-stream streamwise velocity U_∞^*. The temperature T is made nondimensional with respect to the free-stream static temperature T_∞^*. The density ρ, dynamic viscosity μ, and kinematic viscosity ν are made nondimensional with respect to their free-stream values, ρ_∞^*, μ_∞^*, and ν_∞^*, respectively. The free-stream Reynolds number is Re, the free-stream Mach number is M_∞, and the Prandtl number Pr is constant; C_p^* is the specific heat at constant pressure, and κ_∞^* is the free-stream dimensional thermal conductivity. The dynamic viscosity μ^* varies with temperature in accordance with

$$\mu^*=\frac{1.458T^{*3/2}\times 10^{-5}}{T^*+110.4} \qquad \text{for } T^*>110.4\text{ K} \tag{43a}$$

$$\mu^*=0.693873\times 10^{-6}\,T^* \qquad \text{for } T^*\le 110.4\text{ K}, \tag{43b}$$

where μ^* is given in cgs units. The dimensional suction velocity v_w^* is negative for suction and positive for blowing, as is the notation for V_w. The ratio of specific heats γ is constant and equal to 1.4. The nondimensional wall temperature is denoted by T_w, and the nondimensional adiabatic wall temperature is denoted by T_{ad}.

The quasi-parallel inviscid instability equations of the compressible disturbed flow have various forms [2]. In this analysis, we use the form given by

$$D\zeta_1=\frac{i\alpha\rho_m DU_m}{\Gamma}\zeta_1-\left(\frac{\alpha^2+\beta^2}{\Gamma}+\frac{M_\infty^2\Gamma}{\rho_m}\right)\zeta_2 \tag{44}$$

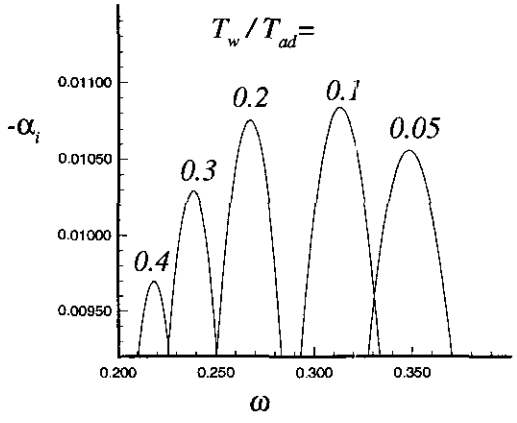

FIG. 2. Variation of the inviscid growth rate of second-mode waves with frequency at $M_\infty = 5$, $T_\infty = 50$ K, and $Pr = 0.72$.

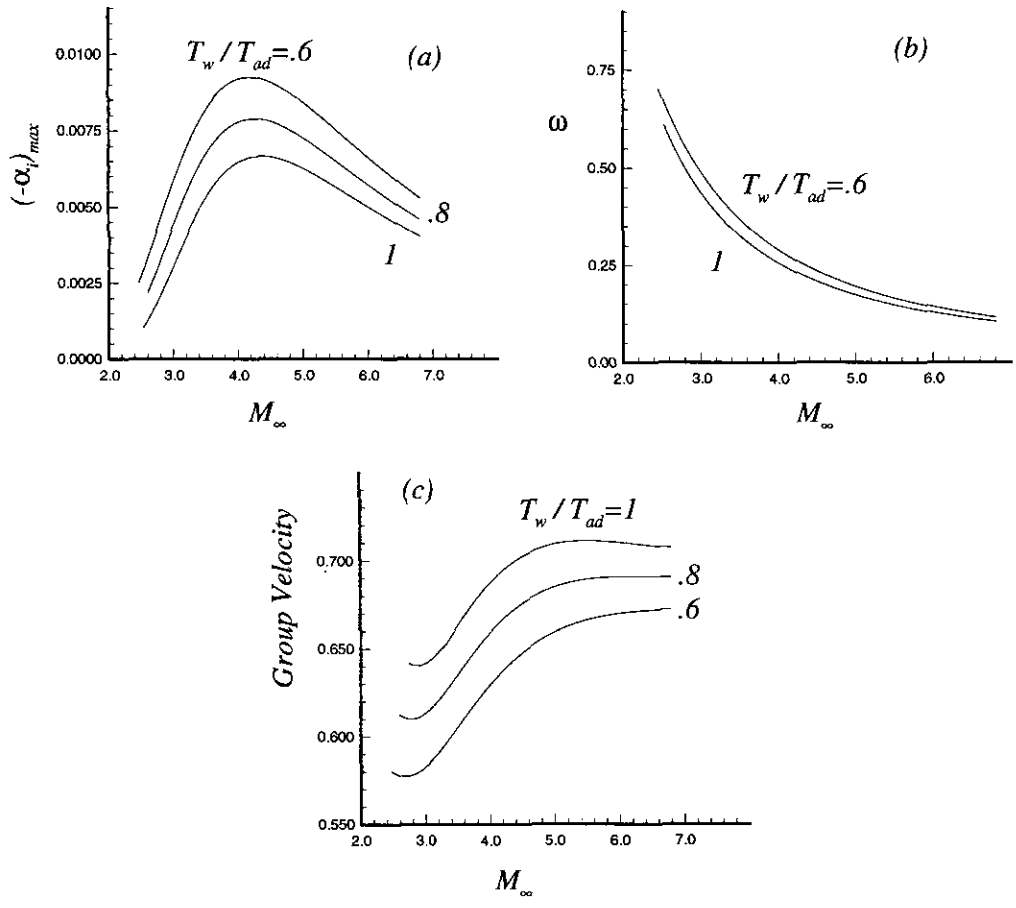

FIG. 3. (a) Variation of maximum growth rate of second-mode inviscid disturbances with Mach number for three levels of heat transfer at T_∞ = 50 K and Pr = 0.72. (b) Corresponding frequencies. (c) Corresponding group velocities.

$$D\zeta_2 = -\Gamma\zeta_1, \tag{45}$$

where $D = d/d\mathrm{y}$,

$$v = \zeta_1 e^{i(\alpha x+\beta z-\omega t)} + cc \tag{46a}$$

$$p = \zeta_2 e^{i(\alpha x+\beta z-\omega t)} + cc \tag{46b}$$

$$\Gamma = -i\rho_m(\omega - \alpha U_m). \tag{47}$$

The boundary conditions at the wall are

$$\zeta_1 = 0 \quad \text{at } y = 0 \tag{48}$$

and in the free-stream, the boundedness of the disturbance requires that

$$\zeta_1 - \left(\frac{\alpha^2+\beta^2}{\Gamma_e^2} + M_\infty^2\right)^{1/2}\zeta_2 = 0 \tag{49}$$

where

$$\Gamma_e = -i(\omega - \alpha) \tag{50}$$

If Eqs. (44), (45), (48), and (49) are differentiated with respect to ω and we assume

$$\xi = \left\{\zeta_1, \zeta_2, \frac{\partial\zeta_1}{\partial\omega}, \frac{\partial\zeta_2}{\partial\omega}, \alpha, \omega\frac{\partial\alpha}{\partial\omega}\right\}^T \tag{51a}$$

and

$$\{\xi\} = \{\xi_1, \xi_2, \xi_3, \xi_4, \xi_5, \xi_6, \xi_7\}^T \tag{51b}$$

then the resulting system, which is coupled with the system of Eqs. (44) and (45), can be rewritten as

$$D\{\xi\} = [G]\{\xi\}, \tag{52}$$

where G is a 7×7 matrix of the corresponding complex elements. The boundary conditions are rewritten as

$$\xi_1 = \xi_3 = 0 \quad \text{at } y = 0 \tag{53}$$

$$\xi_1 - \tau^{1/2}\xi_2 = 0 \quad \text{at } y = y_e \tag{54}$$

and

$$\xi_3 - \tau^{1/2}\xi_4 - \frac{1}{2\tau^{1/2}}\frac{\partial \tau}{\partial \xi_6}\xi_2 = 0 \quad \text{at } y = y_e, \tag{55}$$

where

$$\tau = \frac{\xi_5^2 + \beta^2}{-i(\xi_6 - \xi_5)} + M_\infty^2 \tag{56}$$

and η_e is the value of η at the edge of the boundary layer. Note that we are interested in performing calculations at a constant value of β; therefore, β is not treated as a dependent variable and $\partial\beta/\partial\omega$ is set equal to 0. The system of Eqs. (52) has 14 real differential equations, and Eqs. (53)–(55) offer 8 real boundary conditions. Four real boundary conditions follow from normalization; thus, we let

$$\xi_2 = \xi_4 = 1 \quad \text{at } y = 0. \tag{57}$$

The remaining two boundary conditions follow from using spatial stability ($\omega_i = 0$) and the requirement of the maximum spatial growth rate over all frequencies (i.e., $\partial\alpha_i/\partial\omega = 0$). These conditions are rewritten as

$$\text{Imag}(\xi_6) = 0 \tag{58}$$

$$\text{Imag}(\xi_7) = 0. \tag{59}$$

The system is now closed. The solution procedure and the split into real and imaginary parts follow the approach outlined in the previous application.

We present results for the maximum growth rates over all frequencies of two-dimensional ($\beta = 0$) second-mode disturbances. Mack [2] showed that second-mode disturbances in two-dimensional flows are most amplified when they are aligned with the flow (two-dimensional disturbances). In the

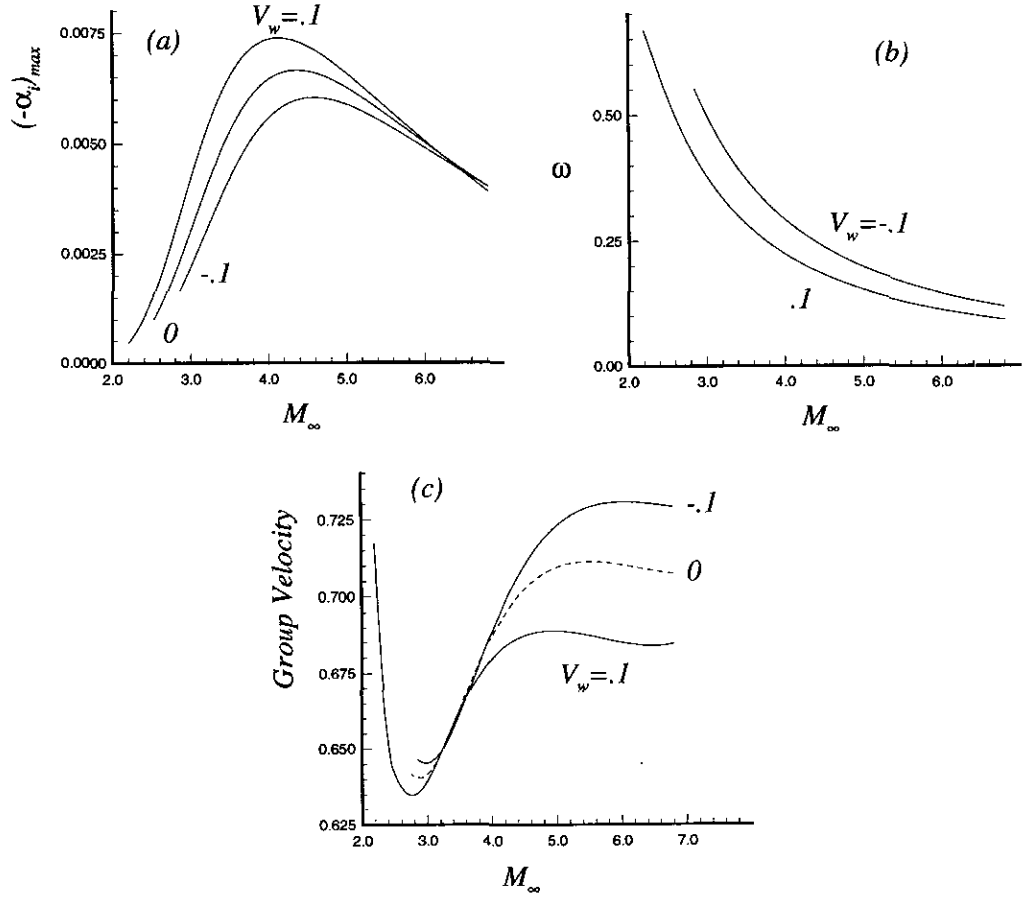

FIG. 4. (a) Variation of maximum growth rate of second-mode inviscid disturbances with Mach number for three levels of self-similar suction at adiabatic conditions, $T_\infty = 50$ K and Pr = 0.72. (b) Corresponding frequencies. (c) Corresponding group velocities.

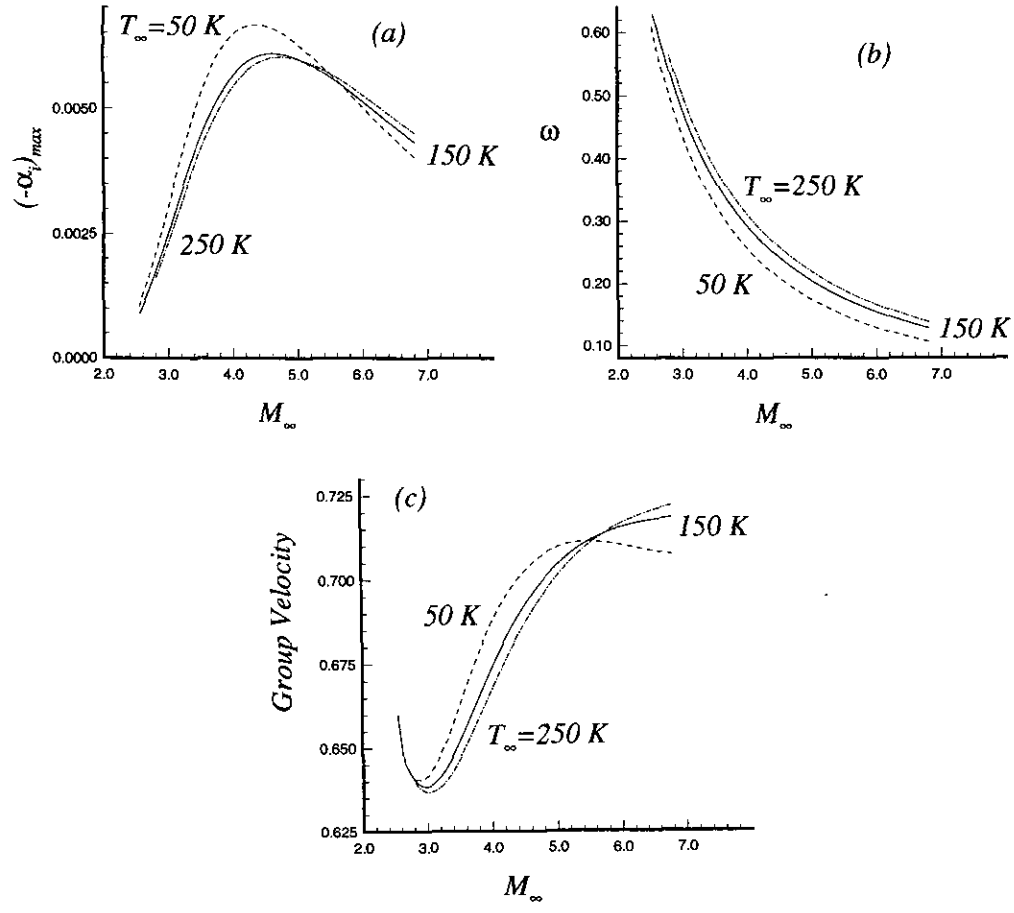

FIG. 5. (a) Variation of maximum growth rate of second-mode inviscid disturbances with Mach number for three freestream temperatures at adiabatic conditions with no suction and Pr = 0.72. (b) Corresponding frequencies. (c) Corresponding group velocities.

results, we present the effects of heat transfer, self-similar suction, and free-stream static temperature on the maximum growth rates of second-mode disturbances at various Mach numbers. The results of the direct computation of the maximum disturbance growth rate are in perfect agreement with the results of the indirect computation.

Cooling destabilizes second-mode disturbances [2], except at large levels [6] of cooling, where the maximum growth rate might actually decrease slightly with cooling (Fig. 2). The results in Fig. 3a show this effect. Figure 3b clearly shows that cooling shifts the maximum growth rate toward a higher frequency. The group velocity of second-mode disturbances (Fig. 3c) decreases with cooling and increases with Mach number (except at Mach numbers smaller than 3, where the first and second modes merge).

In Fig. 4a, we show the effect of self-similar suction and blowing on the inviscid maximum growth rates as a function of Mach number. The figure clearly shows that at moderate Mach numbers suction inviscidly stabilizes second-mode disturbances, although the stabilization is not as large as what is obtained from viscous stability theory. This result is in agreement with the findings of Mack [7]. At relatively large Mach numbers, suction becomes inviscidly destabilizing; blowing is slightly stabilizing. This result indicates that most of the stabilizing effect of suction, particularly at high Mach numbers, is due to viscosity, which agrees with the conclusion of Malik [8]. Figure 4b shows that suction shifts the frequencies that correspond to the maximum growth rates toward higher values, such as the case with viscous calculations. The group velocity (Fig. 4c) increases with suction and decreases with Mach number until the merging region of the first and second modes, where it increases sharply.

The variation of the maximum inviscid growth rate with Mach number for three free-stream temperatures is shown in Fig. 5a. At high Mach numbers, an increase in the free-stream temperature increases the maximum growth rate whereas at relatively low Mach numbers the opposite takes place. Because the inviscid instability problem has, by definition, no viscosity term, then the effect of the free-stream temperature on the stability eigenvalue comes only through its effect on varying the viscosity in the mean flow. Viscous stability calculations performed by Mack [9] at Mach 6.8 show that an increase

in the free-stream temperature has a stabilizing effect. The frequencies that correspond to the maximum growth rates increase as the free-stream temperature increases (Fig. 5b). The group velocities that correspond to the maximum growth rates are shown in Fig. 5c.

4. SUMMARY

A new method that allows direct computation of boundary-layer stability characteristics is presented and applied to two sample problems: the viscous instability of incompressible flow over a flat plate and the inviscid instability of compressible flow over a flat plate. The method, in its general form, can be applied to any differential eigenvalue problem. The method consists of differentiating the original eigenvalue problem with respect to one or more parameters of the dispersion relation. The resulting new problem (or problems) are coupled with the original problem; however, the opposite is not true. Each differentiation of the original problem with respect to a parameter of the dispersion relation introduces an additional dispersion relation. The resulting problem (or problems) can be solved with the original problem simultaneously and with some of the parameters of the dispersion relation treated as dependent variables. The desired characteristic imposes a condition (or conditions) that is used as a boundary condition along with the original, differentiated, and normalization boundary conditions. Several examples demonstrate that the coupled problem is closed.

APPENDIX A

The nonzero elements of matrix $[F]$ in Eq. (22) are

$$f_{12} = 1$$
$$f_{21} = \Gamma$$
$$f_{23} = RDU$$
$$f_{24} = i\alpha R$$
$$f_{31} = -i\alpha$$
$$f_{42} = \frac{-i\alpha}{R}$$
$$f_{43} = -\frac{\Gamma}{R},$$

where

$$\Gamma = \alpha^2 + iR(\alpha U - \omega).$$

APPENDIX B

The nonzero elements of matrix $[H]$ in Eq. (28) are

$$h_{12} = 1$$
$$h_{21} = \Gamma$$
$$h_{23} = RDU$$
$$h_{24} = iR\xi_9$$
$$h_{56} = 1$$
$$h_{61} = \Lambda$$
$$h_{64} = iR\xi_{11}$$
$$h_{65} = \Gamma$$
$$h_{67} = RDU$$
$$h_{68} = iR\xi_9$$
$$h_{71} = -i\xi_{11}$$
$$h_{75} = -i\xi_9$$
$$h_{81} = \frac{i}{R}\xi_{11}$$
$$h_{83} = -\frac{\Lambda}{R}$$
$$h_{85} = -\frac{i}{R}\xi_9$$
$$h_{87} = -\frac{\Gamma}{R},$$

where

$$\Gamma = \xi_9^2 + iR(\xi_9 U - \xi_{10})$$

and

$$\Lambda = 2\xi_9\xi_{11} + iRU\xi_{11} - iR.$$

APPENDIX C

The nonzero complex elements of the complex Jacobian $[J]$ in Eq. (34) are

$$J_{12} = 1$$
$$J_{21} = \Gamma$$
$$J_{23} = RDU$$
$$J_{24} = iR\xi_9$$
$$J_{29} = \xi_1\frac{\partial\Gamma}{\partial\xi_9} + iR\xi_4$$
$$J_{2,10} = \xi_1\frac{\partial\Gamma}{\partial\xi_{10}}$$
$$J_{31} = -i\xi_9$$
$$J_{39} = -i\xi_1$$
$$J_{42} = -\frac{i}{R}\xi_9$$
$$J_{43} = -\frac{\Gamma}{R}\xi_3$$
$$J_{49} = -\frac{i}{R}\xi_2 - \frac{1}{R}\xi_3\frac{\partial\Gamma}{\partial\xi_9}$$
$$J_{4,10} = -\frac{1}{R}\xi_3\frac{\partial\Gamma}{\partial\xi_{10}}$$
$$J_{56} = 1$$
$$J_{61} = \Lambda$$
$$J_{64} = iR\xi_{11}$$
$$J_{65} = \Gamma$$
$$J_{67} = RDU$$
$$J_{68} = iR\xi_9$$
$$J_{69} = \xi_5\frac{\partial\Gamma}{\partial\xi_9} + \frac{\partial\Lambda}{\partial\xi_9} + iR\xi_8$$
$$J_{6,10} = \xi_5\frac{\partial\Gamma}{\partial\xi_{10}}$$
$$J_{6,11} = \xi_1\frac{\partial\Lambda}{\partial\xi_{11}} + iR\xi_4$$
$$J_{71} = -i\xi_{11}$$
$$J_{75} = -i\xi_9$$

$$J_{79} = -i\xi_5$$
$$J_{7,11} = -i\xi_1$$
$$J_{81} = -\frac{i}{R}\xi_{11}$$
$$J_{83} = -\frac{\Lambda}{R}$$
$$J_{85} = -\frac{i}{R}\xi_9$$
$$J_{87} = -\frac{\Gamma}{R}$$
$$J_{89} = -\frac{i}{R}\xi_5 - \frac{1}{R}\xi_7\frac{\partial\Gamma}{\partial\xi_9} - \frac{1}{R}\xi_3\frac{\partial\Lambda}{\partial\xi_9}$$
$$J_{8,10} = -\frac{1}{R}\xi_7\frac{\partial\Gamma}{\partial\xi_{10}}$$
$$J_{8,11} = -\frac{i}{R}\xi_1 - \frac{1}{R}\xi_3\frac{\partial\Lambda}{\partial\xi_{11}},$$

where

$$\Gamma = \xi_9^2 + iR(\xi_9 U - \xi_{10})$$
$$\Lambda = 2\xi_9\xi_{11} + iRU\xi_{11} - iR$$
$$\frac{\partial\Gamma}{\partial\xi_9} = 2\xi_9 + iRU$$
$$\frac{\partial\Gamma}{\partial\xi_{10}} = -iR$$
$$\frac{\partial\Lambda}{\partial\xi_9} = 2\xi_{11}$$
$$\frac{\partial\Lambda}{\partial\xi_{11}} = 2\xi_9 + iRU.$$

ACKNOWLEDGMENTS

The comments of Dr. C. David Pruett are greatly appreciated. This research is supported by the Theoretical Flow Physics Branch, Fluid Mechanics Division, NASA Langley Research Center, Hampton, VA, under Contract NAS1-19299.

REFERENCES

1. M. R. Malik, LST and PSE for boundary-layer transition prediction, in *Proceedings of the First Bombardier International Workshop on Aircraft Icing/Boundary-Layer Stability and Transition,* edited by I. Paraschivoiu, (Sept. 1993).
2. L. M. Mack, Boundary-layer linear stability theory, AGARD Report 709, 1984.
3. M. R. Malik, *J. Comput. Phys.* **86,** 376 (1990).
4. O. R. Asfar, J. A. Masad, and A. H. Nayfeh, *Comput. Fluids,* **18**(3), 305 (1990).
5. V. Pereyra, PASVA3: An adaptive finite difference Fortran program for first order nonlinear, ordinary boundary problems, in *Lecture Notes in Computer Science* (Springer, New York/Berlin, 1976), Vol. 76, p. 67.
6. S. J. Shaw and P. W. Duck, "The inviscid stability of supersonic flow past heated or cooled axisymmetric bodies," *Phys. Fluids A* **4**(7), 1541 (1992).
7. L. M. Mack, On inviscid acoustic mode instability in supersonic shear flows, *Fourth Symposium on Numerical and Physical Aspects of Aerodynamic Flows, Long Beach, CA 1989.*
8. M. R. Malik, *AIAA J.* **27,** 1487 (1989).
9. L. M. Mack, Boundary-layer stability theory, Jet Propulsion Laboratory, Pasadena, CA, Document 900-277, 1969.